*Journal of The Electrochemical Society*, **155** (5) E49-E55 (2008)
0013-4651/2008/155(5)/E49/7/$23.00 © The Electrochemical Society



# Electrochemical Synthesis of Diamondlike Carbon Films

**Aislinn H. C. Sirk*** **and Donald R. Sadoway**,z**

*Department of Materials Science and Engineering, Massachusetts Institute of Technology, Cambridge, Massachusetts 02139-4307, USA*

Electrodeposition of diamondlike carbon films through oxidation of acetylides (prepared both in situ and ex situ) dissolved in dimethylsulfoxide (DMSO) was carried out at room temperature by potentiodynamic, potentiostatic, and galvanostatic methods onto gold substrates. Diamondlike carbon films (and nanoinclusions of diamond, graphite, and lonsdaleite phases) were prepared from acetylene-saturated liquid ammonia at a temperature of −33°C by potentiodynamic, potentiostatic, galvanostatic, and pulsed deposition methods. The films were characterized in situ by electrochemical methods and ex situ by Raman spectroscopy, optical microscopy, transmission electron microscopy, profilometry, and electron diffraction. Films were successfully deposited by both methods. The fastest growth rate was achieved with acetylides prepared ex situ and oxidized in the presence of $NaBH_4$ in DMSO solution. Film thickness was found to increase either by processing at higher values of potential or for longer deposition times. Films of the highest quality and greatest uniformity were prepared by pulsed deposition from acetylene-saturated liquid ammonia. Nanodiamond and lonsdaleite inclusions were obtained by potentiostatic deposition from the same medium.
 [DOI: 10.1149/1.2883729] 

Manuscript submitted August 13, 2007; revised manuscript received November 23, 2007. Available electronically March 13, 2008.

Diamond has many properties that make it attractive as an engineering material. The physical properties of diamond include extreme mechanical hardness (ca. 90 GPa), high wear resistance, high bulk modulus ($1.2 \times 10^{12}$ $Nm^{-2}$), low compressibility ($8.3 \times 10^{-13}$ $m^2$ $N^{-1}$), high room-temperature thermal conductivity ($2 \times 10^3$ $Wm^{-1}$ $K^{-1}$), very low thermal expansion coefficient at room temperature ($1 \times 10^{-6}$ $K^{-1}$), large range of optical transparency [deep ultraviolet (UV) to far infrared (IR)], and high sound propagation velocity (17.5 km $s^{-1}$). Very resistant to chemical corrosion and biologically compatible, diamond surfaces can possess very low or even "negative" electron affinity. With a bandgap energy of 5.4 eV, diamond is a very good electrical insulator.[1]

Currently, thin films of diamond are produced through a variety of chemical vapor deposition (CVD) techniques onto a substrate held at elevated temperatures (ca. 900°C) at very slow growth rates (on the order of microns per hour). The cost is such (<$1.00/carat) that quality films are now being produced commercially for use as die cutters for nonferrous materials. However, if the cost could be lowered further while maintaining quality, applications such as heat conductors to help cool electronics and optics might turn to diamond films.[1] Preparing the films by electrodeposition at ambient or subambient temperatures rather than by high-temperature vapor deposition is thought to be a promising avenue for lowering the costs of diamond and diamondlike thin films. Because electrodeposition is conducted in a liquid, as opposed to a low-density gas, faster deposition rates are anticipated. The equipment required for electrodeposition is much simpler and less expensive than that needed for chemical vapor deposition. Also, electrodeposition is not a line-of-sight process; hence, it is possible to make uniform coatings on objects of irregular shape.

Since Namba first pioneered the concept of electrodeposition from solution (as opposed to gas phase) for production of diamond thin films in 1992,[2] there has been considerable interest and activity in this area. A selection of experimental conditions and characterization techniques is shown in Table I.

As would be expected, the substrate, electrolyte/C source, voltage, and current all affect the properties of the resulting C film. For example, pulsed electrodeposition of dimethylformamide (DMF) at 1600 V gives a higher quality diamondlike carbon film than that produced from methanol or acetonitrile at 600–1600 V or DMF at 600 V.[3] It has been suggested that liquids with a higher dipole moment and dielectric constant produce a more diamondlike film, as do methyl-group-containing organic liquids over those with ethyl groups. This was demonstrated in a comparison that ranked acetonitrile > DMF > nitromethane > methanol > nitroethane > ethanol in terms of ability to generate a more diamondlike film.[4] However, by changing processing conditions others have shown it is possible to obtain high-quality films from ethanol.[5]

The majority of the previous work was carried out at high voltages (tens to thousands of volts), but some work has been carried out at low voltages, including electrodeposition at room temperature from a solution of lithium acetylide prepared in situ in dimethylsulfoxide (DMSO)[6,7] and also from acetic acid in aqueous solutions.[8] Deposition from acetylene-saturated ammonia has also been carried out at low temperatures (−33°C and below).[9-11]

It is believed that in vapor-phase deposition the active species is a $CH_3$ radical, and the mechanism proceeds by deposition of both diamond and graphitic carbon. Concomitantly, excess H radicals are produced that preferentially etch the graphitic phase over the diamond phase.[1] No methods of deposition from solutions have been able to achieve the high quality of diamond film that is possible through CVD. However, methods to increase the population of radicals at the surface of the electrode are very appealing because they may lead to a higher percentage of $sp^3$ vs $sp^2$ carbon.

Raman spectroscopy is the most commonly used method to determine the purity of the deposited films. The most important peaks are the D peak at ~1350 $cm^{-1}$ and the G peak at ~1585 $cm^{-1}$, both due to $sp^2$-hybridized carbon. Pure graphite has a single sharp peak at 1585 $cm^{-1}$ and pure diamond has a single sharp peak at 1332.5 $cm^{-1}$. Raman is an excellent method for observing graphitic impurities in a diamond film, as the Raman signal of $sp^2$-hybridized carbon is 50 times stronger than that of $sp^3$-hybridized carbon.

One significant shortcoming of Raman as a method of characterization is that the Raman spectra of environmental carbon match very closely to that of the deposited films. This weakness is underreported in the literature. In fact, several papers make conclusive statements as to the $sp^3$-to-$sp^2$ ratios of electrodeposited films based on the G/D line ratios despite careful studies[12-14] showing that the G/D line ratios and positions are dependent on many variables, not just the $sp^3$-to-$sp^2$ ratios.

## Experimental

*Synthesis of Li acetylide.— Li acetylide (I).*— 2.85 g LiH (0.36 moles) was added to 106 mL of dry DMSO under argon in a 500 mL four-necked round-bottomed flask fitted with a thermometer, two stopcocks, and a stopper. The flask was placed in a water bath and heated to 60°C under an atmosphere of argon. Once the highly exothermic reaction began, the water-bath temperature was adjusted to keep the reaction temperature between 55 and 60°C. After 3 h, acetylene was bubbled through the dark green solution until no further weight gain was observed, and the resulting viscous

* Electrochemical Society Student Member.
** Electrochemical Society Active Member.
z E-mail: dsadoway@mit.edu

**Table I. Methods of preparation of diamond thin films from room-temperature solutions.**

| Substrate | Anode | Solution | Voltage (V) | Current ($mA/cm^2$) | Characterization | Ref. |
|---|---|---|---|---|---|---|
| Indium tin oxide (ITO) -coated glass | Graphite | DMF, acetonitrile, ethanol, or methanol | 2000 | 4–30 | X-ray photoelectron spectroscopy (XPS), Fourier transform infrared spectroscopy (FTIR), Raman, scanning electron microscopy (SEM) | 44 |
| Si (111) | Graphite | Methanol | 1500 | 20 | SEM, Raman | 35 |
| ITO-coated glass | Graphite | Methanol, DMF, or acetonitrile | 600–1600 (7 kHz, 50%) | 0–70 | Raman, IR, XPS, UV visible spectroscopy (UV-Vis), resistance | 3 and 45 |
| ITO-coated glass | Graphite | Acetonitrile, DMF, nitromethane, methanol, nitroethane, or ethanol | 2000 | 2–30 | Raman, XPS, FTIR, SEM | 4 |
| Si | Pt | Ethanol | 800 | 8 | SEM, Raman, micro-Raman | 5 |
| $SnO_2$-coated glass | Graphite sheet | 0.5–20% acetic acid, water | 0–5000 | 10 mA | Raman, X-ray diffraction (XRD), SEM, bandgap, refractive index | 46 |
| Si (100) | Graphite plate | Methanol, urea (N doped films) | 800–1600 | 15–22 | Raman, XPS, FTIR | 47 |
| Si (111) | Graphite plate | DMSO | 150 | no data | XPS, atomic force microscopy (AFM), FTIR, Raman | 48 |
| Si (100) | Graphite rod | $\alpha$ and $\beta$-pinenes in n- hexanes | No data | 2–3 | XRD, FTIR, Raman, Photoluminescence (PL), XANES | 49 |
| Stainless steel (SS) | SS | DMSO, $LiC_2H$ | 1200, 700 $\mu$F | Pulsed deposition | XPS, AFM, Raman | 50 |
| SS or Ni | Graphite plate | DMSO, t-butyl-$NH_4ClO_4$, $LiC_2H$ | 0.3–2.5 (vs Ag/AgCl) | 1 | Micro-Raman, XPS, Raman, microscopy | 6 |
| Pt-coated $SiO_2$ | Not stated | DMSO, t-butyl-$NH_4ClO_4$, $LiC_2H$ or $H_2O$, $CH_3CO_2H$, $CH_3CO_2Na$,$Na_2SO_4$ | 2 (vs Ag/AgCl) | 2 | Auger, X-ray-excited Auger, XPS | 7 |
| $SnO_2$-coated glass | Graphite sheet | 0.5–1% acetic acid, $H_2O$ | 2–4 | 0.04–0.1 | Raman, bandgap, refractive index, PL, SEM, FTIR | 8 |
| Ni foil | Pt foil | Acetylene-saturated ammonia (−40 to −60°C) | 1.4–6.0 (vs Pt) | 0.1–2.2 | Raman, SEM, XPS, FTIR | 9 |
| Ni, Co, Fe, graphite | Not stated | Acetylene-saturated ammonia (−33 to −70°C) | 2–5 | 1–100 | Raman, ED, SEM, auger | 10 and 11 |

black solution was separated into batches for subsequent use.[6] The dark blue/black color has been observed previously[15] and is attributed to polymerization and oligomerization of excess acetylene.[16] On the assumption of 100% yield, the concentration of Li acetylide in DMSO is calculated to be 3.6 M and is reported as such.

*Li acetylide (II).*— Under argon, 70 mL of 2.0 M n-butyl lithium in hexane was added to 100 mL n-hexane in a three-necked 250 mL round-bottomed flask fitted with a stir bar. The flask was submerged in a salt/ice bath and fitted with a gas inlet, gas outlet, and thermometer. When the flask temperature reached −15°C, acetylene was introduced. The acetylene was previously dried by passing through a concentrated $H_2SO_4$ solution and then through a column containing NaOH pellets, molecular sieves, activated charcoal, and desiccant (as an indicator). The reaction flask was kept below −10°C by periodic addition of liquid nitrogen to the salt/ice bath. Acetylene was added until 30 min had elapsed after the time it first bubbled out of the check valve. The solution was warmed to room temperature and then refluxed to remove any dissolved gases.[17] The resulting white powder ($Li_2C_2$) was filtered, rinsed with hexane, and characterized by IR and Raman spectroscopy. When added to the DMSO solution for electrochemical measurements, the solution would darken over time, eventually becoming a dark viscous solution similar in appearance to the Li acetylide(I) solution after several days.

*Electrochemistry.*— All tests were conducted in a three-electrode cell driven by a Solartron S1 1286 Electrochemical Interface (Solartron Analytical, Oak Ridge, TN) controlled by a PC running CorrWare (Scribner Associates, Southern Pines, NC).

The DMSO solutions were purged with Ar and then blanketed with Ar for the duration of the measurements. The reference electrode was either a Ag/AgCl aqueous electrode or a Ag wire. The counter electrode was a Pt foil. Tetra-n-butyl ammonium perchlorate ($[CH_3(CH_2)_3]_4NClO_4$) was added to the solutions as an electrolyte at a concentration of 0.1 M. The working electrode material varied, the most common being gold, plated on a glass slide (Evaporated Metal Films, Inc., Ithaca, NY) with ~0.5 $cm^2$ exposed to solution. The gold slides were sonicated in an acetone/deionized water solu-

tion, then an optional acetone/deionized water solution containing diamond powder, before rinsing multiple times with acetone and deionized water.

The liquid ammonia solution was prepared by condensing $NH_3$ gas into a four-necked round-bottomed flask. Condensation was carried out using either a Dewar condenser filled with an acetonitrile/liquid nitrogen slurry or a double-walled, high-efficiency condenser through which −40°C ethanol was pumped via a cryostat. The ammonia was maintained as a liquid by continuously refluxing. The supporting electrolyte (when used) was either 0.1 M KI or 0.1 M $CF_3SO_3K$. The reference electrode was a Ag wire (flame cleaned before each run), the counter electrode was a Pt foil, and the working electrode was a gold substrate.

*UV irradiation*.— The UV light source was an Ealing Electro-optics (model 37-4769) deuterium power supply (200–400 nm) set at 250 mA and 65 V. This was focused into a 4 mm diam spot size directly on the electrode surface, which was immersed a few millimeters below the electrolyte solution.

*Raman*.— Raman spectra were collected on a Kaiser Hololab 5000R Raman Spectrometer with Raman Microprobe attachment. The light source was either the 514.5 or 785 nm line produced by Coherent CW Argon-Ion and Ti:S Lasers, respectively. Small fibers guided the light to the specimen, resulting in spot sizes of 5–7 μm. The majority of Raman spectra were collected at 514.5 nm, because this allows better splitting between the G and D peaks. Data were collected using Holograms 4.0 with dark subtract and intensity correction.

*Transmission electron microscopy (TEM)*.— Microstructural characterization of the films was carried out using TEM [TEM JEOL 2010 CX and TEM JEOL 2011], which required that specimens be electrodeposited directly onto a gold TEM grid.

*Profilometry*.— Surface topography and film thicknesses measurements were carried out on a Tencor P-10 Surface Profilometer using a 2 μm radius diamond tipped stylus.

## Discussion and Results (DMSO)

*General film characteristics*.— The significant difference between this study and the majority of previously reported electrosynthesis work (Table I) is the exclusive use of low-voltage techniques (<3.5 V vs Ag wire) herein. Although low-voltage techniques have been employed previously in both DMSO[6,7] and aqueous solutions[8] and from acetylene-saturated ammonia solutions,[9-11] the majority of the work has been done at higher voltages (see Table I, and references therein). In a solution containing only supporting electrolyte (no carbon source), a redox peak is observed at ~1 V, due to gold stripping/deposition. When $Li_2C_2$ is added to the solution, an oxidation peak is observed at a potential exceeding 1.0 V (Fig. 1), which is ascribed to

$$x\ \mathrm{C} \equiv \mathrm{C}^{2-} \rightarrow \mathrm{C}_{2x}(\mathrm{sp}^3 \text{ and } \mathrm{sp}^2) + 2x\ \mathrm{e}^- \qquad [1]$$

No complementary reduction peak associated with the reverse reaction is observed.

The electrodeposited films were generated either galvanostatically or by a controlled potential technique resembling cyclic voltammetry with incrementally increasing switching potential. In all cases, the electrode resistance would increase with current passed as can be observed in Fig. 1, which shows a typical deposition history. The decrease in current with cycling is due to the increase in the charge transfer resistance of the electrode, due to the growth of the resistive film on the surface of the electrode that inhibits further film growth. This decrease in current is not due to a decrease in the concentration of the electroactive species, as evidenced by the fact that the introduction of a fresh electrode would be accompanied by an increase in current to its initial value. In a comparison of films deposited at a constant potential of 1.8 vs 1.3 V, the films deposited at the higher potential were thicker, less uniform, and more friable.

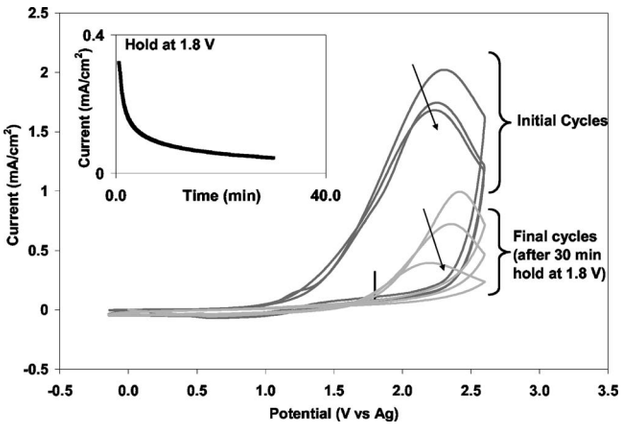


**Figure 1.** Increase in film resistance with electrochemical cycling and holding (Au slide WE, Pt CE, 20 mV/s, 3.6 M $Li_2C_2$, 0.1 M $[CH_3(CH_2)_3]_4NClO_4$, 25 mM $NaBH_4$ in DMSO).

Holding for longer times (60 vs 30 min) at 1.3 V resulted in slightly thicker films (4700 Å as compared to 4300 Å) that retained a uniform appearance.

In a typical deposition (Fig. 1), the electrode potential was cycled, followed by holding at a constant value, and then cycled again to allow electrochemical characterization. Holding the potential (inset in Fig. 1) results in a drop in current over time, and after 30 min, the final characterization cycles show a marked increase in resistance, which is taken as evidence of the formation of an insulating film. Note that significant current is passed on the final cycles only when the applied voltage is higher than the holding voltage. Galvanostatic methods were also used and films with similar characteristics were deposited. However, in this mode, there were issues with voltage spiking at higher current densities and corresponding dissolution of the gold substrate.

*Effect of $NaBH_4$ addition*.— As pure $sp^3$ C is electronically insulating, it is not possible to electrochemically deposit a perfect diamond film of any practical thickness. To address the insularity of diamond, $NaBH_4$ was added to the electrolyte solution with the intention that boron be incorporated into the carbon lattice, resulting in a p-type semiconductor and, therefore, a thicker, somewhat electronically conducting, diamond film. Borane gas has been used as an additive in CVD to successfully prepare highly crystalline conductive diamond films, which have been well characterized electrochemically,[18-25] and tested for several practical uses including oxygen gas evolution in molten chlorides (containing metal oxides).[26]

In Synthesis I, the effect of boron doping was readily observed in the physical appearance of the as-deposited film, which shows more extensive film/particle growth in the presence (Fig. 2a) of boron

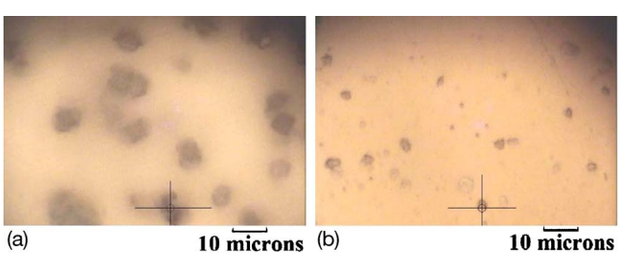


**Figure 2.** (Color online) (a) Multiple cycles to 2.4 V vs Ag wire in 16 mM $NaBH_4$, 3.6 M $LiC_2H$/DMSO, 0.1 M $[CH_3(CH_2)_3]_4NClO_4$, Au slide WE, Pt CE. (b) Multiple cycles to 2.4 V vs Ag wire in 3.6 M $LiC_2H$/DMSO 0.1 M $[CH_3(CH_2)_3]_4NClO_4$, Au slide WE, Pt CE.

**Table II. Effect of deposition conditions on the thickness of the deposited film.**

| Starting material | Boron concentration (samples) | Potential regime (V) | Film Thickness (Å) |
|---|---|---|---|
| Li acetylide (I) | Boron doped | Cycle 2.4 | **1100 ± 160** |
| | No boron doping | Cycle 1.8–2.4 | **870 ± 170** |
| | No boron doping | Hold 1.8 | **1130 ± 140** |
| Li acetylide (II) | Boron doped | Hold 1.8 | **4300 ± 1200** |
| | Boron doped | Hold 1.3 | **4600 ± 1000** |
| | No boron doping | Cycle 1.8 | **3000 ± 1700** |

than in its absence (Fig. 2b). In addition, films deposited in the presence of B were measured to be ~40% thicker than those deposited in its absence (Table II).

Figure 3 shows that the addition of $NaBH_4$ had almost no impact on the electrochemistry of the solution at the onset (see Initial Cycle). Subsequent processing (inset in Fig. 3), however, resulted in the formation of a film of greater thickness and lower resistance (see Final Cycle) than that generated in the absence of $NaBH_4$, consistent with successful incorporation of B into the diamond lattice and formation of a p-type semiconductor. The larger current was not due to direct oxidation of $NaBH_4$, as the electrochemical signal for that reaction looks quite different. Although the source of Li acetylide in the experiments reported in Fig. 3 was Li acetylide (II), the same effect was observed with solutions of Li acetylide produced by Li acetylide (I).

*Effect of the starting materials (acetylide source) on film properties*.— Even though the electrochemistry of Li acetylide solutions was found to be independent of the source of this starting material, there were measurable differences in the resulting carbon films. Specifically, films made from Li acetylide (II) were thicker by almost a factor of 4 under comparable electrodeposition conditions (Table II), visibly distinguishable to the naked eye from films made from Li acetylide (I), yet indistinguishable by the peak positions of the Raman spectra (Fig. 4). The difference in signal strengths between the two samples is attributed to the differences in thickness of the films.

Electrodeposition on electrodes that had been subjected to optional etching by sonication in a diamond powder suspension resulted in the growth of diamondlike deposits in the scratches made by the diamond powder. Evidence for the presence of the $sp^3$ phase can be found in the Raman signal shown in Fig. 5. Unfortunately, even with extended holding times (>10 h), it was not possible to grow a cohesive film of this desired $sp^3$ phase. To ensure that the origin of the measured Raman signal was not embedded diamond powder, unexposed parts of these same gold slides were characterized and the Raman spectra showed no signal for diamond, even in the scratches left by the etching.

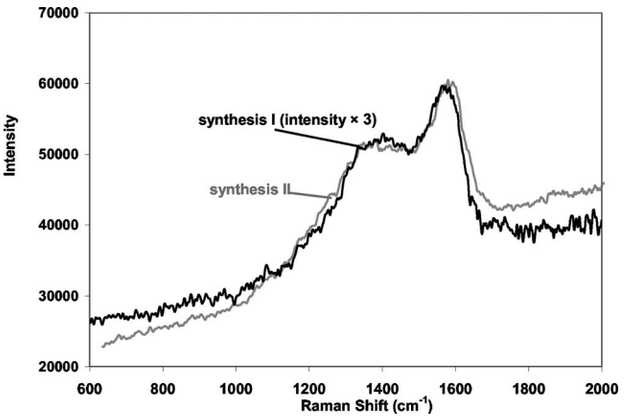


**Figure 4.** Raman spectra (514 nm) of deposited carbon films, Au slide WE, Ag RE, Pt CE, 3.6 M lithium acetylide, 0.1 M $[CH_3(CH_2)_3]_4NClO_4$, 50 mV/s. Processing conditions for trace labeled Synthesis I: Cycling (11 cycles with maximum upper limit 2.2 V). Processing conditions for trace-labeled Synthesis II: Holding (cycle three times to 2.6 V, hold at 1.3 V for 30 min, cycle three times to 2.6 V).

## Discussion and Results ($NH_3$)

Electrochemical deposition of diamondlike carbon films was also carried out from acetylene-saturated liquid $NH_3$, a method used previously by two groups.[9-11] It was hoped that synthesis at low temperature ($NH_3$ boils at −33°C) would allow access to the metastable diamond state. Overall, it appeared that higher-quality films (lower D peak values and appearance of nanodiamond crystals) were produced, but the deposition rate was much slower than that at room temperature in DMSO, and very thin films (barely visible to the naked eye) were deposited.

The source of carbon was acetylene, which when added to liquid ammonia is marked by the appearance of an oxidation peak in the voltammogram, according to

$$x\ HC \equiv CH \rightarrow C_{2x}(sp^3 \text{ and } sp^2) + 2x\ H^+ + 2x\ e^- \qquad [2]$$

Electrolysis of these solutions resulted in the deposition of a diamondlike carbon film confirmed by Raman spectroscopy.

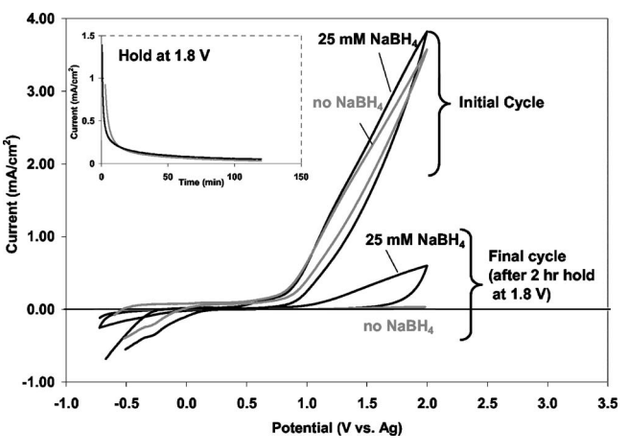


**Figure 3.** Effect of boron doping on the electrochemical response before and after holding for 2 h at 1.8 V (50 mV/s, Au slide WE, Ag ref, Pt CE, 3.6 M $Li_2C_2$, 0.1 M $[CH_3(CH_2)_3]_4NClO_4$).

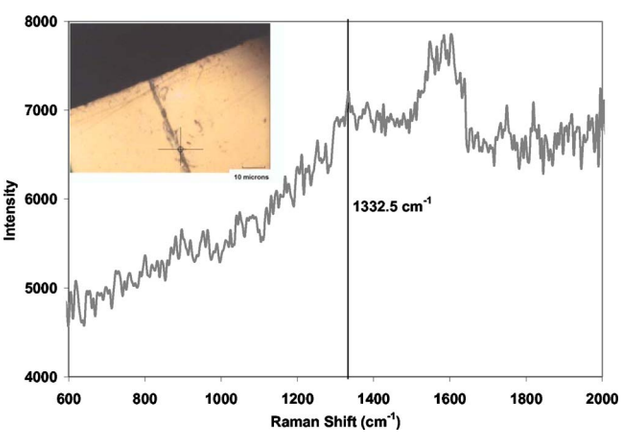


**Figure 5.** (Color online) Raman spectrum (514 nm) of diamond-etched Au slide, multiple cycles to 2.4 V vs Ag wire in 3.6 M $LiC_2H$/DMSO, Au WE, Ag RE, Pt CE, 0.1 M $[CH_3(CH_2)_3]_4NClO_4$.

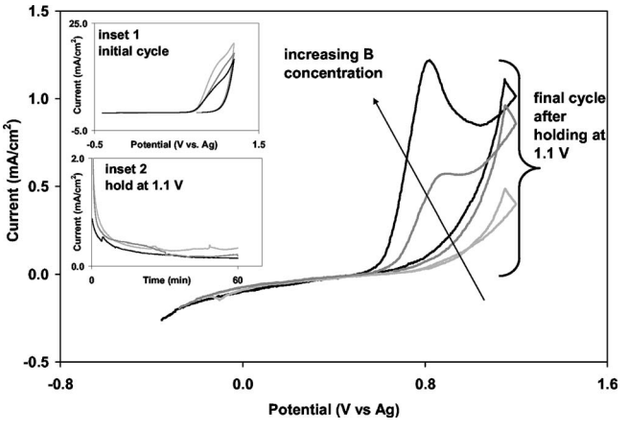


**Figure 6.** Effect of increasing B concentration on the electrochemical behavior [$NH_3$, $C_2H_2$, 0.1 M KI, (0, 23, 46 mM $NaBH_4$) Ag RE, Pt CE, Au WE].

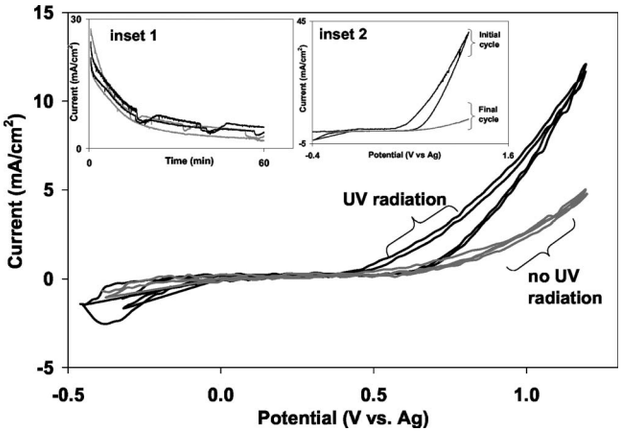


**Figure 8.** Effect of UV radiation on the produced diamondlike carbon films. $NH_3$, $C_2H_2$, Ag RE, Pt CE, Au covered with carbon film WE, 20 mV/s, −33°C. Inset 1: Same electrodes held at 1.1 V. Inset 2: Initial (before holding) and final (after holding) cyclic voltammograms.

*Effect of boron doping*.— The addition of $NaBH_4$ to liquid ammonia had no major impact on the initial electrochemistry (inset 1 in Fig. 6). Even so, films deposited in the presence of $NaBH_4$ were thicker and much more conductive, consistent with successful incorporation of B into the diamond lattice and formation of a p-type semiconductor (Fig. 6). During the oxidation, no evidence of gas formation (associated with nitrogen evolution from the liquid ammonia) was observed.

Raman analysis of the films showed that both the D and G peak positions decrease as the $NaBH_4$ concentration in the electrolyte increases (Fig. 7). This relationship is taken as evidence of B incorporation into the carbon film as is the broadening of the diamond peaks (B doping is tantamount to defect formation in diamond).[22,27]

*Effect of UV radiation*.— In an attempt to generate radicals in the solution in the vicinity of the electrode, focused UV radiation was directed at the electrode surface during electrodeposition. Disappointingly, it was found that films produced under UV photoassist contained a higher proportion of graphitic carbon as evidenced by their higher conductivity than those deposited without radiation (Fig. 8). This is confirmed by the Raman data from these specimens and from specimens prepared in DMSO. It has been observed in CVD (filament assisted) that, if the use of UV radiation did not generate hydrogen radicals, then the growth of the diamond phase was significantly retarded.[28] We speculate that a similar mechanism was at work in our electrochemical system.

*Effect of pulsed potential deposition*.— H radicals can be generated by the reaction of solvated electrons with trace quantities of water.[29] Although dissolution of Li or Na metal in liquid ammonia is the usual method of preparing solvated electrons, electrogeneration also works.[30,31] In this study, the formation potential of solvated electrons was determined to be −2.6 V vs Ag, as confirmed by the presence of a blue cloud at the surface of the electrode.[32,33] The dissipation of the blue cloud with time was attributed to the desired reaction with trace water to form H radicals. It was hoped that the H radicals would preferentially etch the $sp^2$ carbon phase over that of the $sp^3$ carbon phase in a similar mechanism to that of CVD. On a gold working electrode, the voltammetric peak due to reduction of water was measured to lie just slightly more cathodic than −2.0 V,[32] as shown in Fig. 9, which sets forth the expected reaction sequence and shows the pulse conditions in the inset in Fig. 9. Pulsed elec-

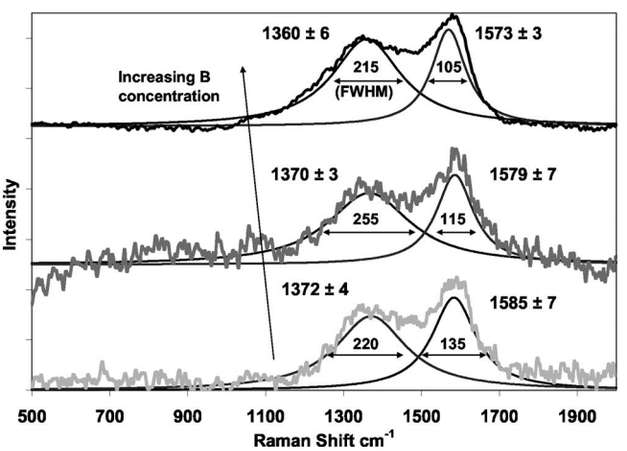


**Figure 7.** Raman spectra (514 nm) showing decrease in D and G peak positions with increasing concentration of B in the electrolyte [$NH_3$, $C_2H_2$, 0.1 M KI, (0, 23, 46 mM $NaBH_4$) Ag RE, Pt CE, Au WE]. Numbers above the peaks are the average of several measurements across the specimen and one standard deviation. Numbers within the peaks are the full-width-half-maximum values for those peaks.

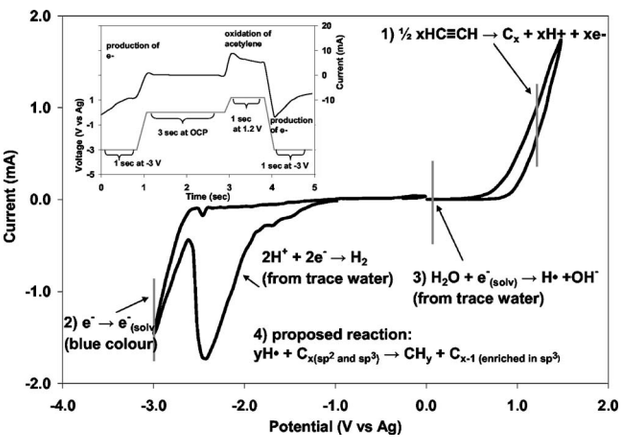


**Figure 9.** Voltammetry of the oxidation of acetylene, reduction of water, and formation of solvated electrons. Inset: Example of carbon film synthesis by controlled-potential pulsing and resulting current response. $NH_3$, $C_2H_2$, Ag RE, Pt CE, Au TEM grid WE, 20 mV/s, −33°C.

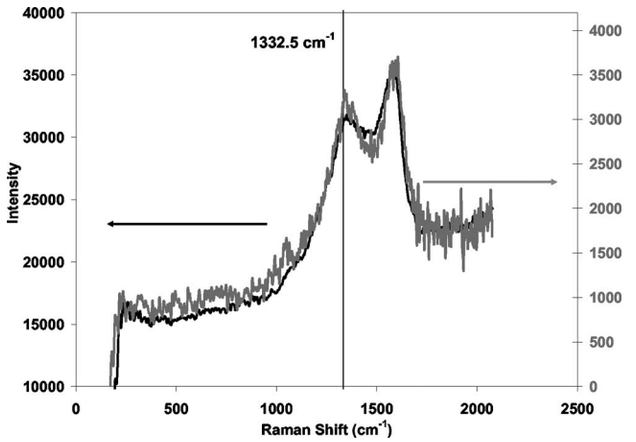


**Figure 10.** Effect of the nature of the applied potential regime on film quality as measured by Raman analysis (514 nm). Pulsed potential electrodeposition (gray); constant potential electrodeposition (black).

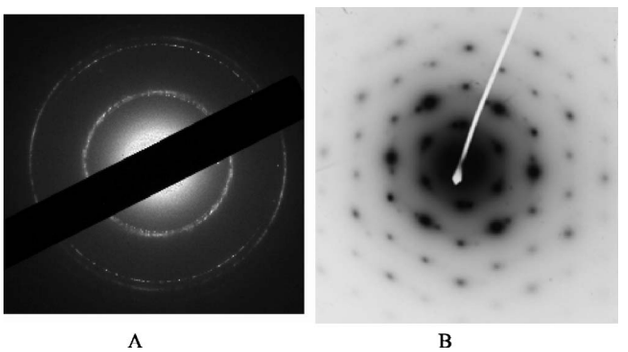


**Figure 11.** (A) Electron diffraction pattern ($NH_3$, $C_2H_2$, Au TEM grid WE, Ag RE, Pt CE, hold 60 min at 1.1 V, UV). (B) Electron diffraction pattern of area showing the crystal structure of single-crystal diamond ( $NH_3$, $C_2H_2$, Au TEM grid WE, Ag RE, Pt CE, hold 60 min at 1.1 V, UV).

trodeposition in this medium produced a film with a higher percentage of $sp^3$ C than films produced by potentiostatic deposition as evidenced by the Raman spectra in Fig. 10.

The pulse regime (a typical one is shown in the inset in Fig. 9) was pulses at −3 V, open circuit potential (OCP), 1.2 V, and back to −3 V. The time at OCP was always 3 s, and the pulse durations at −3 and 1.2 V ranged from 0.001 to 10 s. In the samples prepared with a pulse duration of 0.01 s or less, the resulting film was visible to the naked eye; however, the Raman signal was too weak to interpret. Based on deconvolution of the Raman spectra of the specimens processed at longer pulse durations, a pulse duration of 0.1 s appears to be optimum (assuming that a lower D peak value is indicative of a higher $sp^3$ ratio) with a D peak of 1335 ± 23 $cm^{-1}$ and a G peak of 1546 ± 17 $cm^{-1}$, cf. 1370 ± 2 $cm^{-1}$ and a G peak of 1579 ± 3 $cm^{-1}$ for material generated with 1 s pulses. The larger errors associated with the specimen produced with pulses 0.1 s in duration are attributed to the lower Raman signal strength.

*Nanodiamond.*— Nanocrystallites of diamond have been previously observed in high-voltage deposition from liquids. For example, electrodeposition from pure ethanol at 80 V across a 1 mm electrode gap produced nanodiamond as observed by Raman.[34] On one surface deposited from ethanol at 800 V, there were distinct signals for diamond, diamondlike carbon, polyethylene crystals, and glassy carbon.[5] Micro-Raman spectra of one carbon film corresponded to diamondlike carbon, where the electrode was immersed in solution while samples formed at an air/water interface showed a distinct mix of graphitic carbon and diamondlike carbon.[35]

Bulk analysis by X-ray diffraction (XRD) of our films failed to show any discernable signals for either diamond or graphite, and therefore, TEM and electron diffraction (ED) were used to examine smaller areas and detect smaller crystallites. Results are shown in Fig. 11 and Table III. One of the samples, which had been specially deposited on a TEM grid, showed an ED pattern that corresponded to that of lonsdaleite (or highly strained diamond), including the line at 1.17 Å, which is not seen in natural diamond (except after a diamond is cut[36]). These phases are sometimes observed in artificial diamond, including chemically vapor-deposited films,[37,38] reaction of SiC with $Cl_2$ to prepare diamond structured carbon,[39] and in samples deposited by electron cyclotron resonance plasma at low bias voltages.[40] Lonsdaleite and a 6H diamond polytype were also found when synthesized from various carbon precursors at 2000°C and high pressure using a multianvil apparatus.[41]

In another region of the electrode of the same sample, the electron diffraction pattern for single-crystal diamond (as evidenced by the single spots, as opposed to the rings for a polycrystalline pattern) was observed (Fig. 11). Energy-dispersive spectroscopy analysis of the sample showed the presence of only carbon, gold, and silica (a common contaminant) in the sample.

Electrodeposition of micro- or nanocrystallites of diamond on gold slides was confirmed by micro-Raman spectroscopy as can be seen in Fig. 12. Other measurements across the surface of the de-

**Table III. Diffraction patterns of samples and common carbon phases.**

| | | d spacing [Å] (relative intensity) | | | |
|---|---|---|---|---|---|
| Sample A (polycrystalline) | Sample B (single crystal) | Diamond (pdf no. 01-075-0410) | Lonsdaleite (pdf no. 00-019-0268) | Graphite[a] (pdf no. 98-000-0057) | Gold (pdf no. 98-000-0056) |
| | | | | 3.34 (100) | 2.35 (100) |
| 2.04 (doublet) | 2.05 | 2.06 (100) | 2.18/2.06 (100) | 2.12 (3) 2.03 (17) | 2.04 (52) |
| | | | 1.92 (50) | 1.80 (3) | |
| | | | | 1.67 (6) | |
| | | | 1.50 (25) | 1.53 (5) | 1.44 (32) |
| 1.25 | 1.24 | 1.26 (20) | 1.26 (75) | 1.23 (5) | 1.22 (36) |
| 1.18 | | | 1.17 (50) | 1.15 (8) | 1.18 (12) |
| 1.06 | 1.09 | 1.08 | 1.08 (50) | 1.05 (1) | 1.02 (6) |
| | | | | | 0.94 (23) |
| | | | | | 0.91 (22) |
| | 0.83 | 0.84 | | | 0.83 (23) |
| | | | | | 0.79 |
| | 0.74 | 0.74 | | | 0.72 |

[a] Only selected (the strongest and the ones closest to observed values) graphite lines are listed.

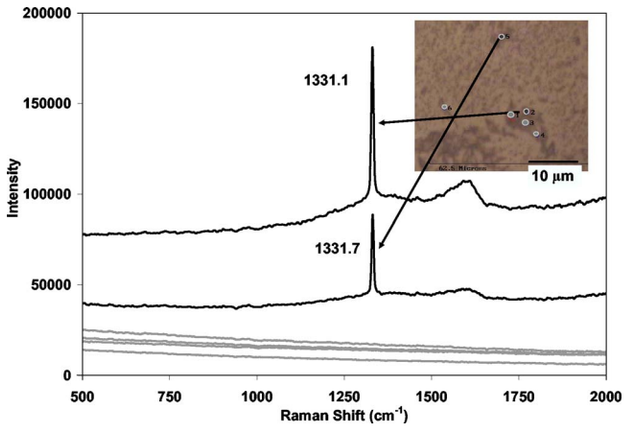


**Figure 12.** (Color online) Raman spectra of sample showing distinct signals due to nanocrystallites of diamond in some regions and very low signals in others ($NH_3$, $C_2H_2$, Au slide WE, Ag RE, Pt CE, hold 60 min at 1.1 V, 0.1 M KI).

posited film confirmed sharp, distinct peaks from 1317 to 1332 $cm^{-1}$, consistent with strained diamond or lonsdaleite.[36,38,42,43] Although the Raman spectrum of bulk diamond is a single line at 1332.5 $cm^{-1}$, the presence of stacking faults arising from strains on the diamond crystal structure can give rise to signals ranging from 1319 to 1333 $cm^{-1}$.[36,38,42,43] These are assigned to various polytypes of diamond. For example, a small side peak at 1322 (Ref. 42) or 1324 $cm^{-1}$ (Ref. 38) observed in CVD diamond film was assigned to a hexagonal diamond polytype as confirmed by X-ray diffraction[38] or reflection.[42] Other measurements have shown this peak can range from 1315 to 1326 $cm^{-1}$,[36] and calculations show that over the full range of diamond polytypes the fine structures of the vibrational spectra will occur below 1332 $cm^{-1}$.[43]

Despite the formation of micro- or nanocrystallites of diamond by several different methods in this study, attempts to grow a uniform pure diamond film electrochemically have been unsuccessful. It was hoped that generating the films under controlled conditions (and possibly with the aid of seeding to enhance film growth) would result in a greater degree of control over film quality. Our results (and those of other groups) are similar to those reported in an earlier stage of diamond synthesis by CVD; yet, high-quality diamond films are presently prepared commercially by that method. Perhaps, with further optimization of processing parameters, it may be possible to achieve the same degree of success in diamond film generation by electrochemical means.

## Acknowledgments

This work was sponsored by the Defense Advanced Research Projects Agency (DARPA) through the Office of Naval Research (ONR) under contract no. N00014-05-1-0895. This work made use of MRSEC Shared Facilities supported by the National Science Foundation under award no. DMR-0213282 and NSF Laser Facility grant no. CHE-0111370.

The authors thank Professor Hongmin Zhu, University of Science and Technology, Beijing, for helpful discussions in connection with the preparation of solutions of liquid ammonia and electrochemical measurements in these media and Elsa Olivetti, MIT, for assistance with TEM measurements.

*Massachusetts Institute of Technology assisted in meeting the publication costs of this article.*

## References

1. P. W. May, *Philos. Trans. R. Soc. London, Ser. A*, **358**, 473 (2000).
2. Y. Namba, *J. Vac. Sci. Technol. A*, **10**, 3368 (1992).
3. K. Cai, D. Guo, Y. Huang, and H. S. Zhu, *Surf. Coat. Technol.*, **130**, 266 (2000).
4. Q. A. Fu, J. T. Jiu, C. B. Cao, H. Wang, and H. S. Zhu, *Surf. Coat. Technol.*, **124**, 196 (2000).
5. Z. Sun, Y. Sun, and X. Wang, *Chem. Phys. Lett.*, **318**, 471 (2000).
6. A. I. Kulak, A. I. Kokorin, D. Meissner, V. G. Ralchenko, I. I. Vlasov, A. V. Kondratyuk, and T. I. Kulak, *Electrochem. Commun.*, **5**, 301 (2003).
7. E. Shevchenko, E. Matiushenkov, D. Kochubey, D. Sviridov, A. Kokorin, and A. Kulak, *Chem. Commun. (Cambridge)*, **2001**, 317.
8. S. Gupta, R. K. Roy, B. Deb, S. Kundu, and A. K. Pal, *Mater. Lett.*, **57**, 3479 (2003).
9. A. M. H. Chen, C. Pingsuthiwong, and T. D. Golden, *J. Mater. Res.*, **18**, 1561 (2003).
10. V. P. Novikov and V. P. Dymont, *Tech. Phys. Lett.*, **23**, 350 (1997).
11. V. P. Novikov and V. P. Dymont, *Appl. Phys. Lett.*, **70**, 200 (1997).
12. A. C. Ferrari and J. Robertson, *Phys. Rev. B*, **64**, 075414 (2001).
13. A. C. Ferrari and J. Robertson, *Phys. Rev. B*, **61**, 14095 (2000).
14. S. Reich and C. Thomsen, *Philos. Trans. R. Soc. London, Ser. A*, **362**, 2271 (2004).
15. J. Kriz, M. J. Benes, and J. Peska, *Tetrahedron Lett.*, **33**, 2881 (1965).
16. J. Kriz, M. J. Benes, and J. Peska, *Collect. Czech. Chem. Commun.*, **32**, 4043 (1967).
17. J. J. Eisch and B. W. Kotowicz, *Eur. J. Inorg. Chem.*, **1998**, 761.
18. M. C. Granger and G. M. Swain, *J. Electrochem. Soc.*, **146**, 4551 (1999).
19. M. C. Granger, M. Witek, J. S. Xu, J. Wang, M. Hupert, A. Hanks, M. D. Koppang, J. E. Butler, G. Lucazeau, M. Mermoux, et al., *Anal. Chem.*, **72**, 3793 (2000).
20. M. C. Granger, J. S. Xu, J. W. Strojek, and G. M. Swain, *Anal. Chim. Acta*, **397**, 145 (1999).
21. T. Kondo, Y. Einaga, B. V. Sarada, T. N. Rao, D. A. Tryk, and A. Fujishima, *J. Electrochem. Soc.*, **149**, E179 (2002).
22. I. Yagi, H. Notsu, T. Kondo, D. A. Tryk, and A. Fujishima, *J. Electroanal. Chem.*, **473**, 173 (1999).
23. M. Yoshimura, K. Honda, T. Kondo, R. Uchikado, Y. Einaga, T. N. Rao, D. A. Tryk, and A. Fujishima, *Diamond Relat. Mater.*, **11**, 67 (2002).
24. M. Yoshimura, K. Honda, R. Uchikado, T. Kondo, T. N. Rao, D. A. Tryk, A. Fujishima, Y. Sakamoto, K. Yasui, and H. Masuda, *Diamond Relat. Mater.*, **10**, 620 (2001).
25. F. J. Del Campo, C. H. Goeting, D. Morris, J. S. Foord, A. Neudeck, R. G. Compton, and F. Marken, *Electrochem. Solid-State Lett.*, **3**, 224 (2000).
26. T. Goto, Y. Araki, and R. Hagiwara, *Electrochem. Solid-State Lett.*, **9**, D5 (2006).
27. S. Ghodbane and A. Deneuville, *Diamond Relat. Mater.*, **15**, 589 (2006).
28. F. G. Celii, H. H. Nelson, and P. E. Pehrsson, *J. Mater. Res.*, **5**, 2337 (1990).
29. U. Schindewolf, in *International Conference on the Nature of Metal–Ammonia Solutions*, J. J. Lagowski and M. J. Sienko, Editors, p. 199, Ithica, NY (1969).
30. E. M. Abbot and A. J. Bellamy, *J. Chem. Soc., Perkin Trans. 2*, **1978**, 254 (1978).
31. D. H. Evans, *Acc. Chem. Res.*, **10**, 313 (1977).
32. R. M. Crooks and A. J. Bard, *J. Phys. Chem.*, **91**, 1274 (1987).
33. A. J. Bard, K. Itaya, R. E. Malpas, and T. Teherani, *J. Phys. Chem.*, **84**, 1262 (1980).
34. K. Sreejith, J. Nuwad, and C. G. S. Pillai, *Appl. Surf. Sci.*, **252**, 296 (2005).
35. M. C. Tosin, A. C. Peterlevitz, G. I. Surdutovich, and V. Baranauskas, *Appl. Surf. Sci.*, **145**, 260 (1999).
36. D. S. Knight and W. B. White, *J. Mater. Res.*, **4**, 385 (1989).
37. M. Frenklach, R. Kematick, D. Huang, W. Howard, K. E. Spear, A. W. Phelps, and R. Koba, *J. Appl. Phys.*, **66**, 395 (1989).
38. S. Bhargava, H. D. Bist, S. Sahli, M. Aslam, and H. B. Tripathi, *Appl. Phys. Lett.*, **67**, 1706 (1995).
39. Y. Gogotsi, S. Welz, D. A. Ersoy, and M. J. McNallan, *Nature (London)*, **411**, 283 (2001).
40. M. Zarrabian, N. Fourches-Coulon, G. Turban, M. Lancin, and C. Marhic, *Diamond Relat. Mater.*, **6**, 542 (1997).
41. N. Dubrovinskaia, L. Dubrovinsky, F. Langenhorst, S. Jacobsen, and C. Liebske, *Diamond Relat. Mater.*, **14**, 16 (2005).
42. L. Fayette, M. Mermoux, B. Marcus, F. Brunet, P. Germi, M. Pernet, L. Abello, G. Lucazeau, and J. Garden, *Diamond Relat. Mater.*, **4**, 1243 (1995).
43. K. E. Spear, A. W. Phelps, and W. B. White, *J. Mater. Res.*, **5**, 2277 (1990).
44. C. B. Cao, H. S. Zhu, and H. Wang, *Thin Solid Films*, **368**, 203 (2000).
45. D. Guo, K. Cai, L. T. Li, and H. S. Zhu, *Chem. Phys. Lett.*, **325**, 499 (2000).
46. R. K. Roy, B. Deb, B. Bhattacharjee, and A. K. Pal, *Thin Solid Films*, **422**, 92 (2002).
47. X. B. Yan, T. Xu, G. Chen, S. R. Yang, and H. W. Liu, *Appl. Surf. Sci.*, **236**, 328 (2004).
48. H. Q. Jiang, L. N. Huang, S. J. Wang, Z. J. Zhang, T. Xu, and W. M. Liu, *Electrochem. Solid-State Lett.*, **7**, D19 (2004).
49. S. C. Ray, B. Bose, J. W. Chiou, H. M. Tsai, J. C. Jan, K. Kumar, W. F. Pong, D. DasGupta, G. Fanchini, and A. Tagliaferro, *J. Mater. Res.*, **19**, 1126 (2004).
50. A. I. Kulak, A. V. Kondratyuk, T. I. Kulak, M. P. Samtsov, and D. Meissner, *Chem. Phys. Lett.*, **378**, 95 (2003).